

# HEATING OF A FULLY SATURATED DARCIAN HALF-SPACE : PRESSURE GENERATION, FLUID EXPULSION, AND PHASE CHANGE

PAUL DELANEY

U.S. Geological Survey, 2255 N. Gemini Dr., Flagstaff, AZ 86001, U.S.A.

(Received 21 April 1983 and in revised form 31 October 1983)

**Abstract**—Analytical solutions are developed for the pressurization, expansion, and flow of one- and two-phase liquids during heating of fully saturated and hydraulically open Darcian half-spaces subjected to a step rise in temperature at its surface. For silicate materials, advective transfer is commonly unimportant in the liquid region; this is not always the case in the vapor region. Volume change is commonly more important than heat of vaporization in determining the position of the liquid-vapor interface, assuring that the temperatures cannot be determined independently of pressures. Pressure increases reach a maximum near the leading edge of the thermal front and penetrate well into the isothermal region of the body. Mass flux is insensitive to the hydraulic properties of the half-space.

## NOMENCLATURE

|      |   |
|------|---|
| $A$  | thermal expansion parameter, $\alpha(T_0 - T_\infty)$   |
| $C$  | heat capacity   |
| $D$  | ratio of penetration depths for thermal and hydraulic diffusion, $\sqrt{(\kappa_l/\omega)}$                         |
| $E$  | ratio of penetration depths for thermal diffusion of liquid- and vapor-filled regions, $\sqrt{(\kappa_l/\kappa_v)}$ |
| $g$  | parameter in Clapeyron equation, defined by equation (9)  |
| $G$  | parameter in nondimensional Clapeyron equation, defined by equation (34)  |
| $h$  | parameter in Clapeyron equation, defined by equation (9)  |
| $H$  | parameter in nondimensional Clapeyron equation, defined by equation (34)  |
| $k$  | absolute permeability   |
| $K$  | thermal conductivity  |
| $L$  | heat of vaporization  |
| $P$  | pressure  |
| $Pe$ | modified Peclet number, defined by equation (32)  |
| $q$  | heat flux   |
| $Q$  | mass flux   |
| $R$  | ratio of properties of vapor to that of liquid (e.g. $R_\mu \equiv \mu_v/\mu_l$ )                                   |
| $St$ | modified Stephan number, $(\rho C)_b(\Delta T)/\phi\rho_l cL$   |
| $t$  | time coordinate   |
| $T$  | temperature   |
| $U$  | internal energy   |
| $v$  | Darcian velocity  |
| $x$  | length coordinate   |
| $X$  | position of liquid-vapor interface.   |

|                    |  |
|--------------------|--|
| $\theta$           | nondimensional temperature, $(T - T_\infty)/(T_0 - T_\infty)$                |
| $\theta_\infty$    | parameter in nondimensional Clapeyron equation, defined by equation (34)     |
| $\kappa$           | thermal diffusivity, $K/(\rho C)_b$  |
| $\lambda$          | position of liquid-vapor interface, $X/\sqrt{(4\kappa_l t)}$                 |
| $\Lambda$          | position of maximum pressure   |
| $\mu$              | dynamic viscosity  |
| $\rho$             | fluid density  |
| $\phi$             | porosity   |
| $\psi$             | nondimensional pressure, $(P - P_\infty)R_\rho k/2\lambda^2 A\kappa_l \mu_v$ |
| $\bar{\psi}$       | nondimensional pressure, $(P - P_\infty)R_\rho k/A\kappa_l \phi \mu_v$       |
| $\bar{\bar{\psi}}$ | nondimensional pressure, $(P - P_\infty)k/A\kappa_l \mu$                     |
| $\psi_\infty$      | parameter in nondimensional Clapeyron equation, defined by equation (34)     |
| $\omega$           | hydraulic diffusivity, $k/\phi\mu\beta$ .                                    |

## Subscripts

|          |   |
|----------|---|
| 0        | value at $x = 0$ or $\eta = 0$                                |
| $\infty$ | value at $x = \infty$ or $\eta = \infty$                      |
| b        | bulk porous composite   |
| c        | value at $x = X$ or $\eta = \lambda$ , on the Clapeyron curve |
| f        | fluid   |
| l        | liquid region   |
| m        | solid matrix  |
| v        | vapor region.   |

## 1. INTRODUCTION

GIBSON *et al.* [1, 2], and Cross *et al.* [3], argue that porous, water-saturated iron-ore pellets can be ruptured by high fluid-pressures generated as a result of intense heating during industrial drying processes. Their equation development, however, is not equivalent to that of Delaney [4], who calculates fluid-pressure increases in water-saturated rocks subjected to intense heating from rapidly emplaced magmas in

## Greek symbols

|          |  |
|----------|--|
| $\alpha$ | thermal-expansion coefficient, $(-1/\rho)(\partial\rho/\partial T)_P$ and equations (4) and (24) |
| $\beta$  | compressibility, $(1/\rho)(\partial\rho/\partial P)_T$   |
| $\zeta$  | normalized Boltzmann coordinate, $\eta/\lambda$  |
| $\eta$   | Boltzmann coordinate, $x/\sqrt{(4\kappa_l t)}$   |

the earth. Delaney [4] treats a hydraulically sealed half-space; conversely, Gibson *et al.* [1, 2], Cross *et al.* [3], and the present paper treat an open half-space. Pressure increases are greatest if the body is initially fully saturated; this situation is considered here. A somewhat similar analysis has been performed to investigate the effects of intense heating of low-permeability concrete walls that are initially only partially water-saturated [5, 6]. The condition of partial saturation, in combination with the low permeability, leads to characteristic hydraulic diffusivities for a vapor-filled material that are less than the thermal diffusivity of concrete. Most rocks, unlithified sediments, soils, and other porous solids have hydraulic diffusivities that are much greater than their thermal diffusivities. The present analysis focuses upon such materials and differs from treatments of drying in porous materials in that hydraulic diffusivity is responsible for migration of the pore fluid, rather than moisture diffusivity [7–10].

Most analyses of heat transfer due to igneous intrusion [11–14] apply in situations when heat transfer is of sufficient duration to generate convective cells. Many igneous processes involve rapid rates of invasion of magma, for which the initial response of ground water is governed by a ‘thermal pressurization’ flow [4] that acts prior to the onset of natural convection. The analysis presented here can be used to estimate maximum pressures generated during sudden intense heating of saturated porous materials, maximum rates of entry of ground water into igneous intrusions, and fluid flux during the initial stages of drying of a porous material, where capillary forces are negligible. An example will be given to estimate the likelihood of fluidization of wet sediments during heat transfer from an invading magma. Emphasis will be placed upon verification of scaling relations for pressures and velocities; presentation of a complete parameter study is beyond the scope of this paper.

## 2. EQUATIONS

Buoyancy effects are neglected, as well as those arising from deformation of the solid matrix of the porous composite. It is assumed that the expulsion of vapor is sufficiently intense that there is no counterflow of air entering from outside the half-space. The fluid can exist in either of two phases; for the problem at hand it can be shown [4, 13] that the liquid and vapor are in contact along a single planar interface so that a two-phase region is not present. Values of nondimensional groups are estimated for situations where the porous matrix is a silicate, the pores are filled with an aqueous fluid, and the difference between the ambient and wall temperature is  $\Delta T \sim 10^2\text{--}10^3$  K.

### 2.1. Field equations

Conservation of mass, momentum, and energy are given by [15, pp. 83, 149–150, 318]

$$\phi \frac{\partial \rho}{\partial t} = - \frac{\partial}{\partial x} \rho v, \quad (1)$$

$$v = -(k/\mu) \frac{\partial P}{\partial x}, \quad (2)$$

$$(\rho C)_b \frac{\partial T}{\partial t} = K \frac{\partial^2 T}{\partial x^2} - (\rho C)_f v \frac{\partial T}{\partial x}. \quad (3)$$

(Inertial, pressure-work and kinetic energy terms were found to be unimportant and are therefore neglected.)

Employing the linear expansions

$$d\rho_v = \rho_0(\beta_v dP - \alpha_v dT), \quad d\rho_l = \rho_\infty(\beta_l dP - \alpha_l dT), \quad (4)$$

and recognizing that the interface between the liquid and vapor regions moves as  $X = X(t)$ , one can write equations for pressure and temperature in the vapor ( $x \leq X$ ) and liquid ( $x \geq X$ ) regions

$$\begin{aligned} \frac{\partial P}{\partial t} - (\alpha_v/\beta_v) \frac{\partial T}{\partial t} \\ = \omega_v \frac{\partial^2 P}{\partial x^2} + \omega_v \left( \frac{\partial P}{\partial x} \right) \left( \beta_v \frac{\partial P}{\partial x} - \alpha_v \frac{\partial T}{\partial x} \right), \end{aligned} \quad x \leq X \quad (5)$$

$$\begin{aligned} \frac{\partial T}{\partial t} = \kappa_v \frac{\partial^2 T}{\partial x^2} + \omega_v \beta_v [\phi(\rho C)_f/(\rho C)_b] \left( \frac{\partial P}{\partial x} \right) \left( \frac{\partial T}{\partial x} \right), \\ x \leq X \quad (6) \end{aligned}$$

$$\begin{aligned} \frac{\partial P}{\partial t} - (\alpha_l/\beta_l) \frac{\partial T}{\partial t} \\ = \omega_l \frac{\partial^2 P}{\partial x^2} + \omega_l \left( \frac{\partial P}{\partial x} \right) \left( \beta_l \frac{\partial P}{\partial x} - \alpha_l \frac{\partial T}{\partial x} \right), \end{aligned} \quad x \geq X \quad (7)$$

$$\begin{aligned} \frac{\partial T}{\partial t} = \kappa_l \frac{\partial^2 T}{\partial x^2} + \omega_l \beta_l [\phi(\rho C)_f/(\rho C)_b] \left( \frac{\partial P}{\partial x} \right) \left( \frac{\partial T}{\partial x} \right), \\ x \geq X \quad (8) \end{aligned}$$

where  $\omega_v$  and  $\omega_l$ , and  $\kappa_v$  and  $\kappa_l$  are thermal and hydraulic diffusivities, respectively. The second terms in the flow equations (5) and (7) contain the parameters  $\alpha/\beta \equiv (\partial P/\partial T)_p$ , which, combined with an appropriate expression for  $\partial T/\partial t$ , accounts for the primary forcing process for pressurization and flow of pore fluid due to accumulation of heat.

### 2.2. Interface equations

Temperature and pressure on the liquid–vapor interface must lie along the Clapeyron curve, which is given by [16, p. 208]

$$P_c = g \exp(-h/T_c). \quad (9)$$

For pure water between 373 and 746 K,  $g = 3.23 \times 10^4$  MPa and  $h = 4.71 \times 10^3$  K, with a maximum error of 0.11 MPa at the critical temperature. The conditions applied at this interface are

$$T(X^-) = T(X^+) = T_c, \quad (10)$$

$$P(X^-) = P(X^+) = P_\infty, \quad (11)$$

$$Q(X^+) - Q(X^-) = -\phi(\rho_{lc} - \rho_{vc}) \frac{\partial X}{\partial t}, \quad (12)$$

$$q(X^+) - q(X^-) = \phi \rho_{lc} L \frac{\partial X}{\partial t}, \quad (13)$$

where mass and heat fluxes,  $Q$  and  $q$ , respectively, are given by

$$Q = \rho v, \quad (14)$$

$$q = -K \frac{\partial T}{\partial x} + UQ. \quad (15)$$

### 2.3. Boundary and initial conditions

Consider the case

$$T(\infty, t) = T_\infty, \quad T(x, t \leq 0) = T_\infty, \quad T(0, t) = T_0, \quad (16)$$

$$P(\infty, t) = P_\infty, \quad P(x, t \leq 0) = P_\infty, \quad P(0, t) = P_0 = P_\infty. \quad (17)$$

The third condition in equation (17) is appropriate for drying and related problems where the wall of the half-space is exposed to the atmosphere. However, it is somewhat arbitrary for problems of igneous intrusion, where pressures depend, in part, upon the hydraulic properties of the invading magma. The condition  $v(0, t) = 0$  has been treated [4] and is probably the more common end-member condition for heating of water adjacent to igneous intrusions. Although the no-flux condition maximizes pore-pressure increases due to heating, the no-pressure condition treated here maximizes velocities.

### 2.4. Nondimensional variables

One can apply the Boltzmann transformation

$$\eta = x/\sqrt{(4\kappa_1 t)}, \quad (18)$$

and infer that the liquid-vapor interface moves as

$$\lambda = X/\sqrt{(4\kappa_1 t)}. \quad (19)$$

For the nondimensional transformed equations to have pressures and pressure gradients in the vapor region that are of order unity, one normalizes  $\eta$  by  $\lambda$

$$\zeta = \eta/\lambda. \quad (20)$$

The nondimensional temperature,  $\theta$ , and pressure,  $\psi$ , are

$$\theta = (T - T_\infty)/(T_0 - T_\infty) \equiv (T - T_\infty)/\Delta T, \quad (21)$$

$$\psi = (P - P_\infty)R_{\rho_c}k/2\lambda^2 A\kappa_1\phi\mu_v, \quad (22)$$

where

$$R_{\rho_c} = \rho_{vc}/\rho_{lc}, \quad (23)$$

$$A = \alpha\Delta T \equiv (-1/\rho_\infty)[(\rho_0 - \rho_\infty)/(T_0 - T_\infty)]_T(T_0 - T_\infty). \quad (24)$$

$1/R_{\rho_c}$  is the volume expansion due to the phase change.

For  $\Delta T > 10^2$  K, one has  $R_{\rho_c} \sim 10^{-3}$ – $10^{-2}$ .  $A$  is the overall volume expansion of the fluid raised through the temperature difference  $\Delta T$  and, therefore, contains contributions from the expansion in the liquid and vapor phases, as well as the phase transition.  $\alpha$  is defined as an *effective* thermal expansion coefficient, obtained by applying a finite-difference approximation over  $\Delta T$ . For  $\Delta T > \sim 10^2$ , we have  $\rho_0 \ll \rho_\infty$ , so that  $\alpha \sim 1/(\Delta T)$  and  $A \sim 1$ .

When recast in terms of  $\zeta$ ,  $\theta$ , and  $\psi$ , equations (5)–(8) are

$$\psi'' + 2D_v^2\lambda^2\zeta\psi' = (\alpha_v/\alpha)R_{\rho_c}\zeta\theta' + (\alpha_v/\alpha)A\theta' \cdot \psi' - 2D_v^2\lambda^2(A/R_{\rho_c})\psi' \cdot \psi', \quad \zeta \leq 1, \quad (25)$$

$$\theta'' + 2E^2\lambda^2\zeta\theta' = -2\lambda^2 Pe_v \psi' \cdot \theta', \quad (26)$$

$$\psi'' + 2D_1^2\lambda^2\zeta\psi' = (\alpha_l/\alpha)(R_{\rho_c}/R_\mu)\zeta\theta' + (\alpha_l/\alpha)A\theta' \cdot \psi' - 2D_1^2\lambda^2(A/R_\mu R_{\rho_c})\psi' \cdot \psi', \quad \zeta \geq 1, \quad (27)$$

$$\theta'' + 2\lambda^2\zeta\theta' = -2\lambda^2 Pe_1 \psi' \cdot \theta', \quad (28)$$

where primes indicate differentiation with respect to  $\zeta$  and

$$D_v = \sqrt{(\kappa_l/\omega_v)}, \quad D_1 = \sqrt{(\kappa_l/\omega_l)}, \quad (29)$$

$$E = \sqrt{(\kappa_l/\kappa_v)}, \quad (30)$$

$$R_\mu = \mu_v/\mu_l, \quad (31)$$

$$Pe_v = (AE^2/R_{\rho_c})[\phi(\rho C)_{lv}/(\rho C)_b],$$

$$Pe_1 = (AR_\mu/R_{\rho_c})[\phi(\rho C)_{ll}/(\rho C)_b]. \quad (32)$$

In general  $R_\mu \sim 10^{-2}$ – $10^{-1}$ ,  $D_1 \ll 1$ , and  $D_v \ll 1$ . Where  $R_{\rho_c} \ll 1$ , one has  $\alpha_v/\alpha \ll 1$  and  $\alpha_l/\alpha \ll 1$ ; where  $R_{\rho_c} \sim 1$ , it is commonly the case that  $\alpha_v/\alpha \sim 1$  and  $\alpha_l/\alpha < 1$ . The term for the accumulation of pressure in the vapor region, the second term on the LHS of equation (25), is sensitive to the normalized vapor diffusion distance  $1/D_v\lambda\zeta \gg 1$ ; the extent of the vapor region is much smaller, so this term is commonly negligible and henceforth neglected. The first two terms on the RHS of equation (25) are both small where the expansion is dominated by the phase change; these terms will be neglected for this case. The last term on the RHS of equation (25) and the last two terms on the RHS of equation (27) are small, and henceforth neglected.

The strength of advective heat transfer is reflected by the Peclet numbers,  $Pe_v$  and  $Pe_1$ , and the position of the liquid-vapor interface,  $\lambda$ . Take  $(\rho C)_b = \phi(\rho C)_l + (1-\phi)(\rho C)_m$ , where  $(\rho C)_m$  is the heat capacity of the matrix material. For siliceous rocks at elevated temperatures,  $(\rho C)_m \simeq 20 \text{ MJ m}^{-3} \text{ K}^{-1}$  [17]. Taking values of water and steam at average temperatures for their respective fields,  $(\rho C)_{lv} \simeq 0.5 \text{ MJ m}^{-3} \text{ K}^{-1}$  and  $(\rho C)_{ll} \simeq 2 \text{ MJ m}^{-3} \text{ K}^{-1}$ . For  $A \sim 1$ ,  $R_\mu \sim 10^{-2}$ ,  $1/R_{\rho_c} \sim 10^3$  and  $\phi \sim 0.1$ , one has  $Pe_v \sim 10^0$  and  $Pe_1 \sim 10^{-1}$ .

The Clapeyron equation (9) transforms to

$$\psi_c = G \exp[-H/(\theta_c + \theta_\infty)] - \psi_\infty, \quad (33)$$

where

$$G = gR_{\rho_c}k/2v^2A\kappa_1\phi\mu_v, \quad H = h/\Delta T,$$

$$\psi_\infty = P_\infty R_{\rho_c}k/2\lambda^2 A\kappa_1\mu_v, \quad \theta_\infty = T_\infty/\Delta T. \quad (34)$$

The interface conditions, equations (10)–(13), transform to

$$\psi(1^-) = \psi(1^+) = \psi_c, \quad (35)$$

$$\theta(1^-) = \theta(1^+) = \theta_c, \quad (36)$$

$$-\psi'(1^-) + (R_\mu/R_{\rho_c})\psi'(1^+) = -(1 - R_{\rho_c})/A, \quad (37)$$

$$-\theta'(1^-) + (1/R_K)\theta'(1^+) - (Pe_v/R_{C_r})\theta_c\psi'(1^-) + Pe_1\theta_c\psi'(1^+) = (2\lambda^2/St)[1 + A\psi'(1^-)], \quad (38)$$

where

$$St = (\rho C)_b(\Delta T)/\phi\rho_{lc}L, \quad (39)$$

$$R_{C_r} = C_{fv}/C_{fl}, \quad (40)$$

$$R_K = K_v/K_l. \quad (41)$$

The parameter  $(1 - R_{\rho_c})/A$  in equation (37) is a ratio of the expansion due to phase change to the overall amount. Commonly, one has  $(1 - R_{\rho_c})/A \sim 1$  and  $1/St < \sim 10^{-1}$ . Thus, for most porous materials and  $\Delta T > \sim 10^2$ , energy consumed in the liquid-vapor phase transition is less important in determining the position of the interface than volume change. In general,  $R_{C_r} \sim 10^{-1}$ , so that the advective component of the heat flux across the interface is important, if  $Pe_v > \sim 10^{-1}$ .

The boundary conditions are

$$\theta(0) = 1, \quad \theta(\infty) = 0, \quad (42)$$

$$\psi(0) = 0, \quad \psi(\infty) = 0, \quad (43)$$

so that the problem is now expressed as two coupled two-point boundary-value problems with a common internal boundary.

### 3. EXPANSION DOMINATED BY PHASE CHANGE

The equations are scaled for situations where the phase change is the dominant mechanism of the expansion of the fluid. The choice of pressure and distance scalings includes the parameter  $\lambda$ , which must be determined from the solution itself. For  $2\lambda^2 Pe_v \ll 1$  and  $2\lambda^2 Pe_1 \ll 1$  the boundary-value problem for the temperature field reduces to Newmann's solution to the Stephan problem

$$\theta = 1 - (1 - \theta_c) \operatorname{erf}(E\lambda\zeta)/\operatorname{erf}(E\lambda), \quad 2\lambda^2 Pe_v \ll 1; \quad \zeta \leq 1, \quad (44)$$

$$\theta = \theta_c \operatorname{erfc}(\lambda\zeta)/\operatorname{erfc}(\lambda), \quad 2\lambda^2 Pe_1 \ll 1; \quad \zeta \geq 1, \quad (45)$$

where  $\theta_c$  is, as yet, undetermined. By straightforward manipulations, pressures are found to be

$$\psi = \psi_c \zeta, \quad \zeta \leq 1 \quad (46)$$

$$\psi = [\psi_c + A_1 R_{\rho_c}/2\lambda^2 A R_\mu (1 - D_1^2)] \operatorname{erfc}(D_1\lambda\zeta)/\operatorname{erfc}(D_1\lambda)$$

$$- [A_1 R_{\rho_c}/2\lambda^2 A R_\mu (1 - D_1^2)] \operatorname{erfc}(\lambda\zeta)/\operatorname{erfc}(\lambda), \quad \zeta \geq 1, \quad (47)$$

where

$$A_1/A = (\alpha_l/\alpha)\theta_c, \quad (48)$$

measures the importance of thermal expansion within the liquid region to the overall expansion. To a good approximation  $1 - D_1^2 \approx 1$  for most plausible values of  $D_1$ , and  $E \approx 1$ . These simplifications are used henceforth. Expansion in the fluid region may be significant because, if  $A_1 R_{\rho_c}/A R_\mu$  is not necessarily much less than 1, one finds that  $\psi \approx \psi_c \operatorname{erfc}(D_1\lambda\zeta)/\operatorname{erfc}(D_1\lambda)$  for  $\zeta > \sim 1$ . These approximations reveal that maximum pressures are attained at the liquid-vapor interface, that there is a rapid flow of vapor from the interface to the outside of the half-space, and that there is a slow flow of vapor into the isothermal regions of the half-space.

Equations (46) and (47) are differentiated and inserted into the equations for conservation of mass and energy at the liquid-vapor interface. Ignoring small terms in equation (47), one finds

$$\psi_c = (1 - R_{\rho_c})/A \approx 1, \quad (49)$$

$$(1 - \theta_c) \exp(-\lambda^2)/\operatorname{erfc}(\lambda) - R_K \theta_c \exp(-\lambda^2)/\operatorname{erf}(\lambda) = (\sqrt{\pi}\lambda/St)(1 + A\psi_c), \quad (50)$$

which must be solved in conjunction with the nondimensional Clapeyron equation. Equation (49) verifies that nondimensional pressure and pressure gradients in the vapor region are indeed of order unity.

As a good simplifying approximation appropriate for many situations, let  $1/St = 0$  and  $R_K = 1$ , so that equation (50) is satisfied by  $\theta_c = \operatorname{erfc}(\lambda)$ . Then,  $\lambda$  can be determined from the Clapeyron equation  $\psi_c \approx 1 = G \exp[-H/(\theta_c + \theta_\infty)] - \psi_\infty$ , which is rewritten with the new variable

$$\bar{\psi} = 2\lambda^2\psi = (P - P_\infty)R_{\rho_c}k/A\kappa_1\phi\mu_v, \quad (51)$$

to yield

$$\bar{\psi}_c \approx 2\lambda^2 = \bar{G} \exp[-H/(\operatorname{erfc}(\lambda) + \theta_\infty)] - \bar{\psi}_\infty, \quad (52)$$

where the Clapeyron parameter,  $g$ , and ambient pressure parameter,  $P_\infty$ , have been rescaled in the same manner as equation (51). Using values of  $g$  and  $h$  for pure water and atmospheric initial conditions,  $\lambda$  varies only with  $R_{\rho_c}k/\kappa\phi\mu_v$  and  $\Delta T$ . This is shown in Fig. 1, where it is shown that  $\lambda^2 > \sim 10^{-1}$  for most situations of interest.

Where expansion of the fluid is dominated by the phase change, the mass flux from the half-space is

$$Q_0 = (\rho_0\phi A\lambda^2/R_{\rho_c})\sqrt{(\kappa/t)}\psi'_0 \approx \rho_\infty\phi\lambda^2\sqrt{(\kappa/t)}. \quad (53)$$

In contrast to the maximum pressure, which is sensitive to hydraulic properties, mass flux from the half-space is independent of relative permeability,  $k/\mu_v$ , even though

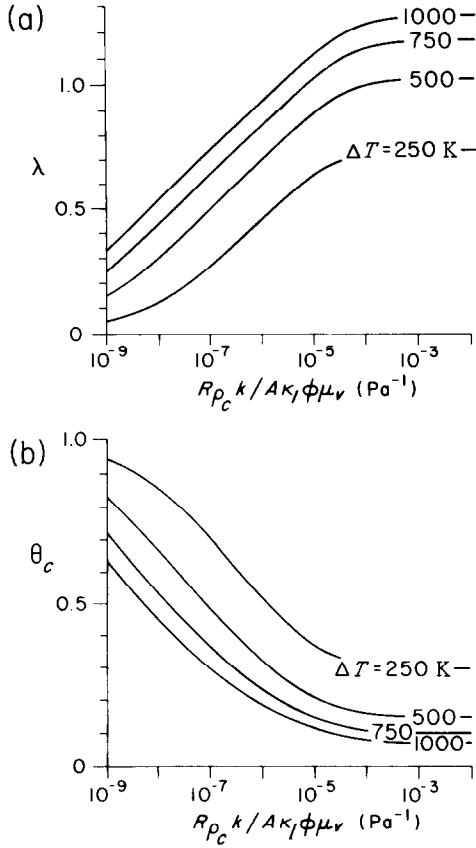


FIG. 1. (a) Interface position,  $\lambda$ , vs  $R_{\rho_c} k / A \kappa \phi \mu_v$  for various  $\Delta T$ . (b) Clapeyron temperature,  $\theta_c$ , vs  $R_{\rho_c} k / A \kappa \phi \mu_v$  for various  $\Delta T$ . Atmospheric initial conditions,  $T_\infty = 300$  K and  $P_\infty = 0.1$  MPa, are used.

the flow is Darcian, implying that rates of drying due to Darcian flow may not be easily distinguishable from drying by other diffusive mechanisms.

Equation (52) offers a relatively simple solution for pressure increases due to heating of hydraulically open bodies subject to heating and is a valid approximation where  $R_{\rho_c} \ll 1$ ,  $2\lambda^2 Pe_v \ll 1$  and  $2\lambda^2 Pe_l \ll 1$ . This is not always the case, and we now treat some related problems.

#### 4. EXPANSION DOMINATED BY PHASE CHANGE, WITH ADVECTION

For many situations  $Pe_v \sim 1$ . It therefore appears that the restriction  $2\lambda^2 Pe_v \ll 1$  may severely constrain the applicability of the solution presented above. For instance, if  $\Delta T = 750$  K and  $R_{\rho_c} k / A \kappa \phi \mu_v = 10^{-6} \text{ Pa}^{-1}$ , then one can find from Fig. 1 that  $\lambda = 0.8$ , so that  $2\lambda^2 = 1.3$ , and advective transfer is found to be a nonnegligible heat-transfer process. However, for  $R_{\rho_c} \ll 1$ , one has  $A_v/A \ll 1$ , and the linear pressure distribution in the vapor region can be inserted into the energy equation (26) to yield

$$\theta'' + 2\lambda^2(\zeta + Pe_v \psi_c)\theta' = 0, \quad \zeta \leq 1, \quad (54)$$

which has the solution

$$\begin{aligned} \theta = 1 - (1 - \theta_c) \{ & \text{erf} [\lambda(\zeta + Pe_v \psi_c)] \\ & - \text{erf} (\lambda Pe_v \psi_c) \} / \{ \text{erf} [\lambda(1 + Pe_v \psi_c)] \\ & - \text{erf} (\lambda Pe_v \psi_c) \}, \quad \zeta \leq 1. \end{aligned} \quad (55)$$

For  $A = 1$  and  $R_{\rho_c} \ll 1$ , the interface equation for mass shows that  $\psi_c = 1$ . The interface equation for energy and the Clapeyron equation show that

$$\begin{aligned} \theta_c = e^{-\lambda^2(1 + Pe_v)^2} \text{erfc}(\lambda) \cdot \{ & e^{-\lambda^2(1 + Pe_v)^2} \text{erfc}(\lambda) \\ & + [\sqrt{\pi} \lambda (Pe_v / R_{\rho_c}) \text{erfc}(\lambda) + e^{-\lambda^2}] \\ & \times [\text{erf} [\lambda(1 + Pe_v)] - \text{erf} (\lambda Pe_v)] \}^{-1} \\ = H / \ln [(1 + \psi_\infty) / G] - \theta_\infty. \end{aligned} \quad (56)$$

For the case  $2\lambda^2 Pe_v \ll 1$ , it was found that  $\lambda$ ,  $\psi_c$  and  $\theta_c$  vary with  $\Delta T$  and  $R_{\rho_c} k / A \kappa \phi \mu_v$  for any given initial conditions. The severity of this constraint is tested by considering the additional parameters  $Pe_v$  and  $R_{\rho_c}$ . For the case  $Pe_v = 1$  and  $R_{\rho_c} = 0.4$ , equation (56) is solved for  $\lambda$ , for various values of  $\Delta T$ , and  $R_{\rho_c} k / A \kappa \phi \mu_v$  in Fig. 2. It is clear that  $\lambda$  is reduced in comparison to the case  $Pe_v \ll 1$ . Temperatures and pressures in the thermal region are shown for various  $Pe_v = 0$  and 1, and  $R_{\rho_c} k / A \kappa \phi \mu_v = 10^{-7} \text{ Pa}^{-1}$  in Fig. 3. For the case  $\Delta T = 750$  K and  $R_{\rho_c} k / A \kappa \phi \mu_v = 10^{-6} \text{ Pa}^{-1}$ , Fig. 2 shows that  $\lambda = 0.5$ , about 40% less than for the case where advective transfer is neglected.

#### 5. EXPANSION NOT DOMINATED BY PHASE CHANGE

Conditions can be such that the phase change is not the dominant mechanism of expansion of the fluid. It is thus of interest to consider the case  $R_{\rho_c} \simeq 1$  and  $1/St = 0$ . Where fluid expansion is dominated by the phase change, the term on the RHS of equation (39) dominates the conservation of mass on the interface; here that term is negligible.

Temperature is given by  $\theta = \text{erfc}(\lambda \zeta)$ . Ignoring

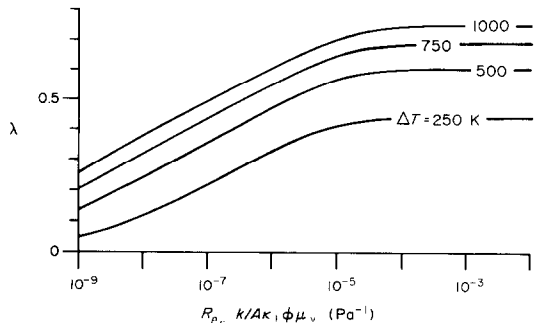


FIG. 2. Interface position,  $\lambda$ , vs  $R_{\rho_c} k / A \kappa \phi \mu_v$  for various  $\Delta T$ .  $Pe_v = 1$ ,  $R_{\rho_c} = 0.4$ ,  $T_\infty = 300$  K and  $P_\infty = 0.1$  MPa.

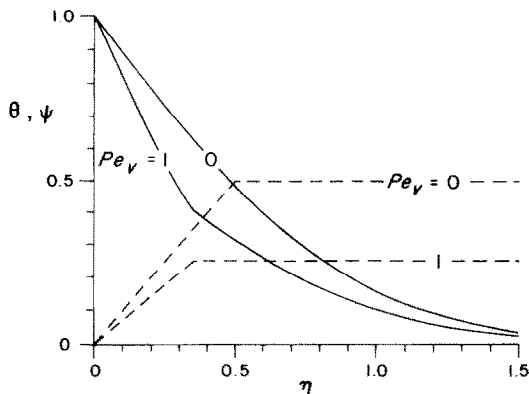


FIG. 3. Temperature (—) and pressure (---) distributions within the thermal region.  $\Delta T = 500$  K,  $R_{Cr} = 0.4$ ,  $R_{pe}k/A\kappa\phi\mu_v = 10^{-7}$ , and atmospheric initial conditions ( $T_\infty = 300$  K and  $P_\infty = 0.1$  MPa).

nonlinear terms, pressures are given by

$$\bar{\psi} = [\bar{\psi}_c - (\alpha_v/\alpha) \operatorname{erf}(\lambda)]\zeta + (\alpha_v/\alpha) \operatorname{erf}(\lambda\zeta), \quad \zeta \leq 1, \quad (57)$$

$$\bar{\psi} = [\bar{\psi}_c + (\alpha_l/\alpha R_\mu) \operatorname{erfc}(\lambda)] \operatorname{erfc}(D_1\lambda\zeta) / \operatorname{erfc}(D_1\lambda) - (\alpha_l/\alpha R_\mu) \operatorname{erfc}(\lambda\zeta), \quad \zeta \geq 1. \quad (58)$$

Expanding  $\operatorname{erfc}(D_1\lambda\zeta)$  and  $\operatorname{erfc}(D_1\lambda)$  in equation (58) and inserting into the interface equation (38), one finds

$$\begin{aligned} \bar{\psi}_c - (\alpha_v/\alpha) \operatorname{erf}(\lambda) + (2\lambda\alpha_v/\sqrt{\pi\alpha}) \exp(-\lambda^2) \\ = -(2D_1\lambda/\sqrt{\pi}) [\bar{\psi}_c R_\mu + (\alpha_l/\alpha) \operatorname{erfc}(\lambda)] / \\ [1 - (2D_1\lambda/\sqrt{\pi})] + (2\lambda\alpha_l/\sqrt{\pi\alpha}) \exp(-\lambda^2). \end{aligned} \quad (59)$$

Noting that the maximum pressure is at, or very near, the phase boundary, one can select  $\lambda = \Lambda$ , so that  $\bar{\psi}_c = \bar{\psi}_{\max}$ , and the Clapeyron equation does not enter into the solution. In this instance, the pressure gradient on each side of the interface must be zero, so that each side of equation (59) is set equal to zero, yielding

$$\begin{aligned} \bar{\psi}_{\max} = (\alpha_v/\alpha) [\operatorname{erf}(\Lambda) - (2\Lambda/\sqrt{\pi}) e^{-\Lambda^2}] \\ = (\alpha_l/\alpha R_\mu D_1) [(1 - 2D_1\Lambda/\sqrt{\pi}) \exp(-\Lambda^2) \\ - D_1 \operatorname{erfc}(\Lambda)]. \end{aligned} \quad (60)$$

Note that  $\Lambda$  depends only upon  $(\alpha_v/\alpha_l)R_\mu$  and  $D_1$ . In general, one finds that  $10^{-2} < (\alpha_v/\alpha_l)R_\mu < 10^0$  and  $10^{-4} < D_1 < 10^{-1}$ .  $\Lambda$  is shown as a function of  $D_1$  and  $(\alpha_v/\alpha_l)R_\mu$  in Fig. 4(a). The relation between  $\bar{\psi}_{\max}/(\alpha_v/\alpha)$  and  $\Lambda$  is shown in Fig. 4(b). It is apparent that  $\Lambda > \sim 2$  for most situations of interest. Where this is the case  $\alpha_v/\alpha = 1$  and the pressure scaling,  $(P - P_\infty)k/A\kappa\phi\mu_v$ , yields nondimensional values that are of order unity. The Peclet number for the thermal region is  $Pe \simeq A[\phi(\rho C)_{lv}/(\rho C)_b]$ , which is commonly small.

## 6. THERMAL EXPANSION WITHOUT PHASE CHANGE

Conditions of heating can be such that a phase transformation does not occur. If  $\theta_c \geq 1$ , the half-space

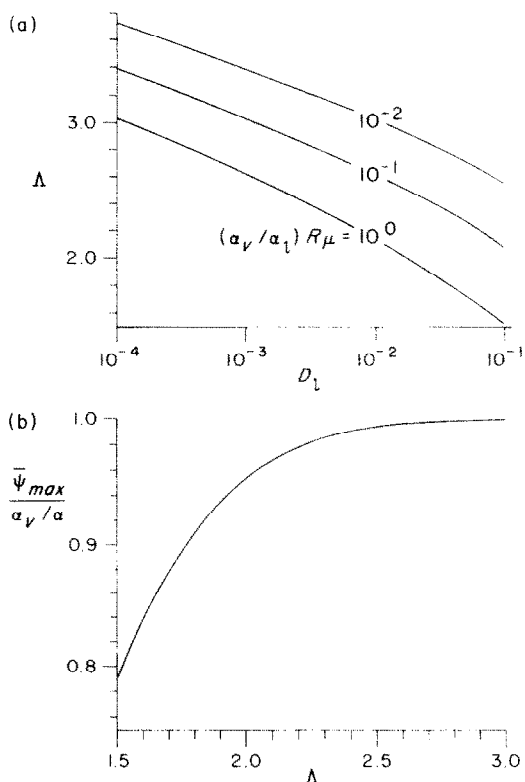


FIG. 4. (a) Position,  $\Lambda$ , of maximum pressure vs  $D_1$  for various  $(\alpha_v/\alpha_l)R_\mu$ . (b) Normalized maximum pressure,  $\bar{\psi}_{\max}/(\alpha_v/\alpha) (\sim \bar{\psi}_{\max})$ , vs  $\Lambda$ .

is filled entirely with liquid; if  $\theta_c \leq 0$ , with vapor. In either case, the Clapeyron and interface equations can be neglected, and the subscripts v and l are dropped from the field equations. We use the Boltzmann variable  $\lambda$ , rather than the normalized variable  $\zeta$ , and the pressure scaling  $\bar{\psi} = (P - P_\infty)k/A\kappa\phi\mu = (P - P_\infty)\beta/AD^2$ . For  $Pe \ll 1$  and  $A \ll 1$ , pressures are given by

$$\bar{\psi} = \operatorname{erf}(\eta) - \operatorname{erf}(D\eta), \quad A \ll 1. \quad (61)$$

For  $\Delta T < \sim 10^2$  K, one has  $A \ll 1$ , and neglect of the second term on the RHS of equation (25) is justified. This pressure distribution, and its associated velocity distribution is shown for various values of  $D$  in Fig. 5. For the common situation of  $D \ll 1$ , the size of the thermal region is negligibly small ( $\sim 1$ ) in comparison to the hydraulic region ( $\sim 1/D$ ). Outside of the thermal region,  $\eta \gg 1$ , pressures are well approximated by  $\bar{\psi} \simeq \operatorname{erfc}(D\eta)$ . The region of greatest interest for drying processes is the thermal region,  $\eta < \sim 1$ , where  $\bar{\psi} \simeq \operatorname{erf}(\eta)$ . For  $D \ll 1$  and  $\eta \gg 1$ , we have  $v \simeq \phi AD\sqrt{(\kappa/\pi t)} \exp(-D^2\eta^2) \simeq 0$ . Within the thermal region,  $\eta < \sim 1$ , we have  $v \simeq -\phi A\sqrt{(\kappa/\pi t)} \exp(-\eta^2)$ . For  $D < \sim 10^{-3}$ , the nondimensional velocities are approximately independent of  $D$  and velocities are negligibly small outside the thermal region.

Differentiating equation (61) and setting  $v = 0$ , one obtains an expression for  $\Lambda$ , the value of  $\eta$  where

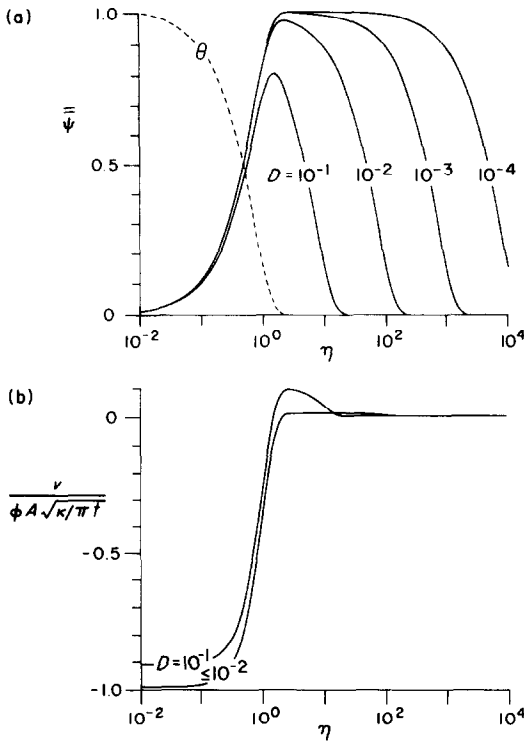


FIG. 5. Semi-logarithmic graphs of nondimensional pressure and velocity vs Boltzmann coordinate,  $\eta$ , for  $A \ll 1$ . (a) Pressure for  $D = 10^{-1}$ ,  $10^{-2}$ ,  $10^{-3}$ , and  $10^{-4}$ . (b) Velocity for  $A \ll 1$  and  $D = 10^{-1}$  and  $10^{-2}$ . Dashed line in (a) is nondimensional temperature.

$$\bar{\psi} = \bar{\psi}_{\max}$$

$$\Lambda = \sqrt{(-\ln(D)/(1-D^2))}. \quad (62)$$

For  $D = 10^{-1}$ , a relatively large value, one has  $\Lambda = 1.53$ ; for  $D = 10^{-2}$ , one has  $\Lambda = 2.15$ . Noting that  $\text{erfc}(2) \approx 0$ , typical values of  $D$  ( $\ll 1$ ) yield maximum pressures outside the thermal region,  $\eta > \sim 2$ .

### 6.1. Numerical results

The above results are valid for  $Pe \ll 1$  and  $A \ll 1$ . To test these approximations, equations (27) and (28) were integrated numerically. Numerical solutions for the special case  $Pe = A = 0$  are in agreement with the analytic solution given above.

Numerical results are summarized in Fig. 6, where  $\Lambda$ ,  $\bar{\psi}_{\max}$ , and the normalized mass flux at  $x = 0$  are plotted against  $D$ , for  $A \ll 1$  and  $A = 1$ , and  $Pe \ll 1$  and  $Pe = 0.1, 1$ .  $\Lambda$  varies with  $A$  [Fig. 6(a)] and is approximately independent of  $Pe$ , so that the position of the maximum pressure as given by equation (61) for  $A \ll 1$  is only about 0.1 greater than for  $A = 1$  and  $Pe \ll 1$ . Thus, numerical integration of the coupled transport equations indicates that the maximum pressure occurs outside the thermal region ( $\Lambda > \sim 2$ ) for  $D < \sim 10^{-2}$ . Maximum nondimensional pressure [Fig. 6(a)]  $\bar{\psi}_{\max}$  can exceed unity by as much as 40% if  $Pe \ll 1$  and  $A = 1$ . If  $Pe \sim 1$  and  $A = 1$ , then  $\bar{\psi}_{\max}$  is of order unity for  $D < \sim 10^{-2}$ , a result that is

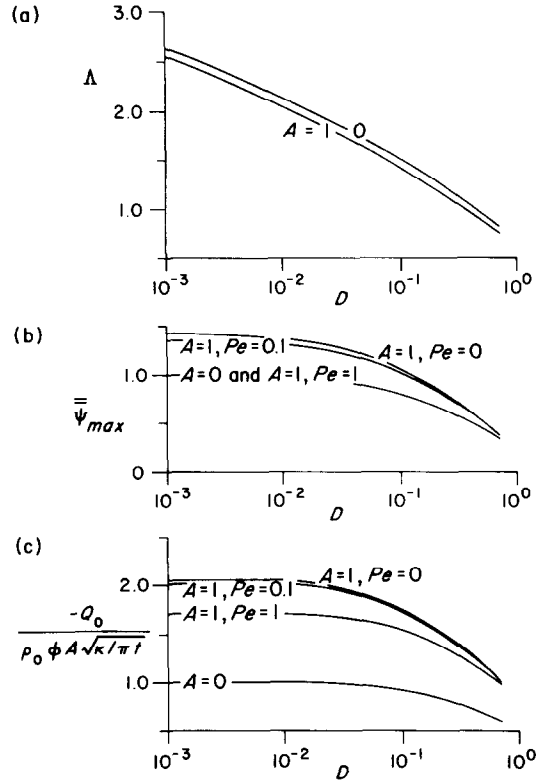


FIG. 6. Comparison of analytic ( $A \ll 1$ ) and numerical results ( $A = 1$ ;  $Pe = 0, 0.1$ , and  $1$ ) vs  $D$ . (a) Position,  $\Lambda$ , of maximum pressure.  $\Lambda$  does not vary substantially with  $Pe$ . (b) Maximum pressure,  $\bar{\psi}_{\max}$ .  $\bar{\psi}_{\max}$  is approximately equal for cases  $A = 0$ , and  $A = 1$  and  $Pe = 1$ . (c) Mass flux,  $Q_0$ .

approximately the same as the analytic solution for  $Pe \ll 1$  and  $A \ll 1$ . In general, however, the analytical solution for  $A \ll 1$  underpredicts the pressure increase due to heating by as much as 40%. The effect of increasing values of  $Pe$  is to reduce the rate of heat transfer into the half-space and therefore to reduce the thermally generated pressure increases. The rate of fluid expulsion from the half-space [Fig. 6(b)] can be  $\sim 100\%$  greater for  $A = 1$  and  $Pe \ll 1$ , than for  $A \ll 1$  and  $Pe \ll 1$ .

## 7. DISCUSSION

After the onset of heating, fluids within the half-space first undergo a slow pressure increase and flow slowly away from the heat source. As the pressure attains its maximum value, the fluid stops flowing. The fluid is then heated and accelerates toward the wall of the half-space as it expands and changes phase during its flow through the thermal region. The velocity contrast at the phase boundary is of the order of the volume change at that boundary. For the purposes of making order-of-magnitude estimates of the above parameters, results provided by the analytical solutions, above, are adequate. To obtain more precise values, governing equa-

tions that include effects of temperature-dependent properties should be integrated numerically.

The condition of a hydraulically open half-space ( $P_0 = P_\infty$ ) maximizes the flow rates due to heating of the pore fluid. The condition of a hydraulically sealed half-space ( $v_0 = 0$ ) maximizes the pressure increase due to heating [4]. In the former case, maximum pressures as well as mass flux are found to be sensitive to properties of the vapor region and  $R_{\rho_c}$  and insensitive to  $\beta$ , so that  $\Delta P \sim 2\lambda^2 A \kappa \phi \mu_v / R_{\rho_c} k$ . In the latter case, maximum pressures are found to be insensitive to properties of the liquid region and  $R_{\rho_c}$  and sensitive to  $\beta$ , so that  $\Delta P \sim AD/\beta = A/(\kappa \phi \mu_l / \beta k)$ . Although not treated here,  $\beta$  is found to be a property of the pore fluid and porous matrix for most rocks and unlithified earth materials [4]. This effect can be included without sacrificing the analytical nature of the results presented above.

It has been postulated by Kokelaar [19] that heat transfer during intrusion of magma gave rise to fluidization of nearby uncemented sediments. For  $\kappa = 10^{-6} \text{ m}^2 \text{ s}^{-1}$ ,  $\phi = 0.3$ ,  $A = 1$ ,  $\Delta T = 750 \text{ K}$ , and  $R_{\rho_c} = 10^{-3}$ , one finds that  $\lambda = 0.5$  for

$$k/\mu_v = \sim 3 \times 10^{-10} \text{ m}^2 \text{ Pa}^{-1} \text{ s}^{-1}.$$

Using  $\mu_v = 4 \times 10^{-5} \text{ Pa s}$ , we find that  $\Delta P < \sim 1 \text{ MPa}$ , for  $k < \sim 10^{-14} \text{ m}^2$ . After 1 h of heat transfer, the maximum velocity of steam is  $\sim 2 \times 10^{-3} \text{ m s}^{-1}$ , sufficient to fluidize quartz grains with diameters less than  $\sim 3 \times 10^{-2} \text{ mm}$  [20]. This is a very fine grained sediment, and most of those described by Kokelaar are coarser. Even if pressure increases are sufficient to overcome the overburden pressure and boundary conditions which maximize velocities are achievable, it still appears that fluidization of the extent and by the process postulated by Kokelaar is an unlikely occurrence restricted to extremely fine-grained materials.

## 8. CONCLUSIONS

A theory for Darcian flow due to thermal pressurization of pore fluids has been developed and solved for the case of a stepwise temperature increase at the surface of a fully saturated, hydraulically open half-space. There are two primary driving parameters for pressurization and flow. The first is  $A = \alpha \Delta T$  ( $\sim 1$ ), which reflects the overall expansion of the fluid heated through  $\Delta T$ ; the second is  $R_{\rho_c} = \rho_{vc}/\rho_{lc}$  ( $\ll 1$  for near-atmospheric pressures), which is the expansion due to the change of phase. These driving terms are generated through the rate of heating of the porous material, which is primarily sensitive to thermal diffusivity. Thus, the rate of drying by a Darcian flow mechanism is proportional to the rate of advance of the thermal front. Maximum pressures, however, are found to lie near or outside the leading edge of the thermal front, so that the mechanical effect of heating penetrates further into the porous material than the heat itself.

The simplest analytical solution is for heating in the

absence of a phase change. In this instance, if  $\Delta T < \sim 10^2 \text{ K}$ ,  $A$  is indeed much less than 1 and the pressure increase is  $\sim AD^2/\beta \equiv A \kappa \phi \mu/k$ . If  $\Delta T > \sim 10^2 \text{ K}$ , then  $A$  is commonly  $\sim 1$  and there is a contrast in properties between the fluid in the thermal and hydraulic regions. In this instance the pressure increase is  $\sim A \kappa \phi \mu_v/k$ . For the important case where the phase change is the dominant mechanism of expansion, it is found that the heat of vaporization is not a significant energy sink. In this instance, the pressure increase is  $\sim 2\lambda^2 A \kappa \phi \mu_v / R_{\rho_c} k$ , where  $\lambda$  is given in Figs. 1 and 2. Analysis reveals that although advected heat is commonly negligible in the liquid region, it can be significant in the vapor region. Because many parameters, especially permeability, vary over many orders of magnitude among different materials, and because of the great number of parameters that otherwise must be included in the analysis, emphasis has been placed upon verification of pressure and velocity scalings summarized above.

*Acknowledgements*—I thank George Homsy of Stanford University and D. J. Andrews of the U.S. Geological Survey for helpful discussions.

## REFERENCES

1. R. D. Gibson, M. Cross and R. W. Young, Pressure generation during the drying of iron ore pellets, *Proc. Int. Conf. on Applied Numerical Modelling*, pp. 539–548. Pentach Press, Southampton (1977).
2. R. D. Gibson, M. Cross and R. W. Young, Pressure gradients generated during the drying of porous shapes, *Int. J. Heat Mass Transfer* **22**, 827–830 (1979).
3. M. Cross, R. D. Gibson and R. W. Young, Pressure generation during drying of a porous half-space, *Int. J. Heat Mass Transfer* **22**, 47–50 (1979).
4. P. T. Delaney, Rapid intrusion of magma into wet rock: groundwater flow due to pore-pressure increases, *J. Geophys. Res.* **87**, 7739–7756 (1982).
5. A. Dayan and E. L. Glueckler, Heat and mass transfer within an intensely heated concrete slab, *Int. J. Heat Mass Transfer* **25**, 1461–1468 (1982).
6. A. Dayan, Self-similar temperature, pressure and moisture distributions within an intensely heated porous half space, *Int. J. Heat Mass Transfer* **25**, 1469–1476 (1982).
7. A. V. Luikov, *Heat and Mass Transfer in Capillary Porous Bodies*. Pergamon Press, Oxford (1966).
8. L. N. Gupta, An approximate solution of the generalized Stefan problem in a porous medium, *Int. J. Heat Mass Transfer* **17**, 313–321 (1974).
9. S. H. Cho, An analytic solution of the coupled phase change problem in a porous medium, *Int. J. Heat Mass Transfer* **18**, 1139–1142 (1975).
10. M. D. Mikhailov, Exact solutions of the temperature and moisture distributions in a porous half space with moving evaporation front, *Int. J. Heat Mass Transfer* **18**, 797–804 (1975).
11. L. M. Cathles, Analysis of the cooling of intrusions by ground-water convection which includes boiling, *Econ. Geol.* **72**, 804–826 (1977).
12. D. Norton and J. Knight, Transport phenomenon in hydrothermal systems: cooling plutons, *Am. J. Sci.* **277**, 937–981 (1977).
13. E. M. Parmentier, Two-phase natural convection adjacent to a heated vertical surface in a permeable medium, *Int. J. Heat Mass Transfer* **22**, 849–855 (1979).
14. E. M. Parmentier and A. Schedl, Thermal aureoles of

- igneous intrusions: some possible indications of hydrothermal convective cooling, *J. Geol.* **89**, 1–22 (1981).
15. R. B. Bird, W. E. Stewart and E. D. Lightfoot, *Transport Phenomena*. Wiley, New York (1960).
  16. D. Tabor, *Gases, Liquids and Solids*. Penguin Books, Baltimore, Maryland (1969).
  17. H. J. Ramey, Jr., W. E. Brigham, H. K. Chen, P. G. Atkinson and N. Arihara, Thermodynamic and hydrodynamic properties of hydrothermal systems, Stanford Geothermal Program Report SGP-TR-6, Stanford University, Stanford, California, 76 pp. (1974).
  18. H. S. Carslaw and J. C. Jaeger, *Conduction of Heat in Solids*. Oxford University Press, London (1959).
  19. B. P. Kokelaar, Fluidization of wet sediments during the emplacement and cooling of various igneous bodies, *J. Geol. Soc. London* **139**, 21–33 (1982).
  20. J. M. Coulson, J. F. Richardson, J. R. Backhurst and J. H. Harker, *Chemical Engineering* (3rd edn.), Vol. 2. Pergamon Press, Oxford (1978).

#### CHAUFFAGE D'UN DEMI-ESPACE COMPLETEMENT SATURE: GENERATION DE PRESSION, EXPULSION DE FLUIDE ET CHANGEMENT DE PHASE

**Résumé**—Des solutions analytiques sont développées pour la pressurisation, expansion et écoulement de fluide liquide ou diphasique pendant le chauffage d'un demi-espace pleinement saturé, hydrauliquement ouvert et darcyen, soumis à un échelon de température à sa surface. Pour des matériaux silicate, le transfert advectif est généralement sans importance dans la région liquide; ceci n'est pas toujours le cas dans la région de vapeur. Un changement de volume est généralement plus important que la chaleur de vaporisation dans la détermination de la position de l'interface liquide-vapeur, assurant que les températures ne peuvent pas être déterminées indépendantes des pressions. Les accroissements de pression atteignent un maximum près du bord d'attaque du front thermique et pénètrent bien dans la région isotherme. Le flux massique est insensible aux propriétés hydrauliques du demi-espace.

#### ERWÄRMUNG EINES VOLLSTÄNDIG GESÄTTIGTEN HALBRAUMES NACH DARCY: DRUCKAUFBAU, FLÜSSIGKEITSAUSTREIBUNG UND PHASENWECHSEL

**Zusammenfassung**—Analytische Lösungen werden für die Verdichtung, Entspannung und Strömung von Ein- oder Zweiphasenflüssigkeiten während des Aufheizens von vollständig gesättigten und hydraulisch offenen Darcy-Halbräumen entwickelt, die an ihrer Oberfläche einem Temperatursprung unterworfen werden. Für Silikate ist der Advektivtransport gewöhnlich im Flüssigkeitsgebiet unbedeutend, was im Dampfgebiet nicht immer der Fall ist. Bei der Bestimmung der Position der Flüssigkeits-Dampf-Grenzfläche ist die Änderung des Volumens gewöhnlich wichtiger als die Verdampfungswärme, wenn die Temperaturen nicht unabhängig von den Drücken bestimmt werden können. Der Druckanstieg erreicht ein Maximum an der "Anströmkante" der Wärme front und setzt sich weit in das isotherme Gebiet des Körpers fort. Der Massenstrom ist gegen die hydraulischen Eigenschaften des Halbraumes unempfindlich.

#### НАГРЕВ ПОЛНОСТЬЮ НАСЫЩЕННОГО ДАРСОВО ПОЛУПРОСТРАНСТВА: СОЗДАНИЕ ДАВЛЕНИЯ, ВЫТЕСНЕНИЕ ЖИДКОСТИ И ИЗМЕНЕНИЕ ФАЗ

**Аннотация**—Получены аналитические решения для процессов создания давления, расширения и течения одно- и двухфазных жидкостей при нагревании полностью насыщенных и гидравлически открытых дарсовых полупространств при ступенчатом увеличении температуры на границе. В силикатных материалах адвективный перенос обычно незначителен в жидкой фазе, но существенен в паровой. Для определения положения границы раздела жидкость-пар более важно изменение объема, чем теплоты парообразования, свидетельствуя о том, что температура и давление должны измеряться одновременно. Возрастающее давление достигает максимального значения у передней кромки теплового фронта и распространяется через стенку в изотермическую область тела. Гидравлические характеристики полупространства не оказывают влияния на величину потока массы.